

Quantifying Spectral Sensitivity Mismatch Using a Metameric Color Rule

David R. Wyle[^]

Avian Rochester LLC, PO Box 1210, Webster, NY, 14580, USA
E-mail: dave@avianrochester.com

Roy S. Berns

Rochester Institute of Technology, 54 Lomb Memorial Dr., Rochester, NY, 14623, USA

Abstract. A new camera metric is proposed based, in concept, on the vision test devised by Davidson and Hemmendinger. The “D&H Color Rule” is a set of two linear patch arrays containing at most one match for near-normal color observers. The match selected by an observer can provide an indication of how that observer’s color vision relates to others. Comparisons may be made to a group of interest, or more commonly, to a CIE Standard Observer. For this research, two image targets have been created, one physical and one virtual, each with a family of spectra related in much the same way as the colors in the original D&H Rule. These targets can be physically imaged or virtually modeled to predict camera RGB, and then CIELAB with a color profile. The camera can then be judged as to what degree its output matches that of a CIE Standard Observer. © 2018 Society for Imaging Science and Technology. [DOI: 10.2352/J.ImagingSci.Technol.2018.62.5.050402]

1. INTRODUCTION

The performance of digital cameras can be evaluated using numerous methods, which should be relevant for each given imaging application. For many applications, the ability of the camera and software systems to accurately predict imaged colors is critical. Other uses for the digital data might be to predict chemical concentrations, to detect the presence of contaminants, etc. Ultimately, in all cases the output camera signals must be related to a set of known input samples. Unknown samples are then assumed to be similarly related to their respective camera output signals. When the application is accurate color, the final metric is how closely the camera replicates the perception of a human, and some additional concerns arise.

Traditionally, the reference color or reflectance of a calibration target is measured, and then the same target is imaged with a test camera. A mathematical relationship is derived between the output digital counts (usually RGB coordinates) and the reference color or reflectance data. This process has been standardized by the International Color Consortium [1] through the use of device profiles. Once a profile is created, arbitrary test charts can be imaged,

and the camera color output can be compared with the measurements for those charts in order to verify the profile accuracy. The comparison is made using one or more color difference formulas and statistical measures such as mean, maximum, and/or a specific percentile.

The literature has described several metrics for evaluating spectral sensitivities [2]. Vora and Trussell [3] proposed an approach where a camera’s spectral sensitivity is compared to a set of color matching functions, based on an idea first proposed by Neugebauer [4]. The Vora and Trussell metric, “ μ factor,” is similar to a correlation coefficient where a value of unity defines a camera having spectral sensitivities which are a linear transformation of color matching functions. There are three limitations to this metric. First, it has non-intuitive magnitudes that may not predict perception. Second, it does not take into account the improvement in color accuracy through profiling. That is, the metric is based solely on the spectral sensitivities, while actual camera performance is generally improved by profiling, such as that described by the ICC [1]. Third, it requires knowledge of a camera’s spectral sensitivities, which require specialized apparatus and experimental skill to properly measure.

The approach proposed here is to use the tools already in place for camera characterization, but to apply a method that has traditionally been limited to the evaluation of human color vision. One potential advantage of this approach is that it may serve as a generalized evaluation target rather than material specific targets.

2. THE D&H COLOR RULE

The D&H Color Rule, [5] produced by Davidson and Hemmendinger, is a color vision test used successfully for decades [6]. It relies on two sets of color patches, each consisting of a family of similar spectra. The observer under test adjusts the position of the two sets of patches until the best color match is found. When viewed by a near-normal observer, there will be only one such match. To judge the metameric effect of a pair of light sources, the observer should make another match under a second light source. The degree of closeness of the two matches is an indication of nearness of the colorimetric renderings of the light source pair. Similarly, two different observers can make a match

[^] IS&T Member.

Received Apr. 14, 2018; accepted for publication July 23, 2018; published online Aug. 28, 2018. Associate Editor: Chunghui Kuo.

1062-3701/2018/62(5)/050402/6/\$25.00

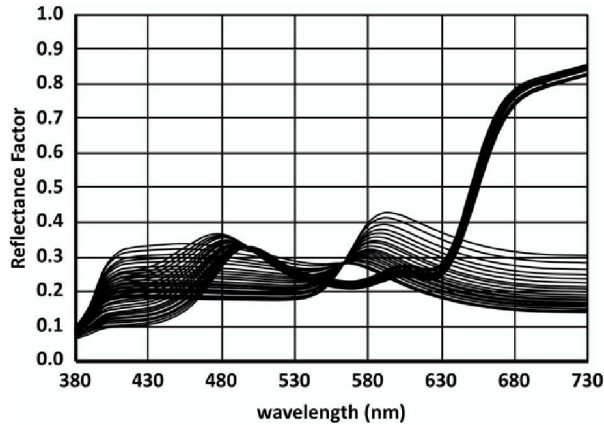


Figure 1. Spectral reflectance of a D&H Color Rule.

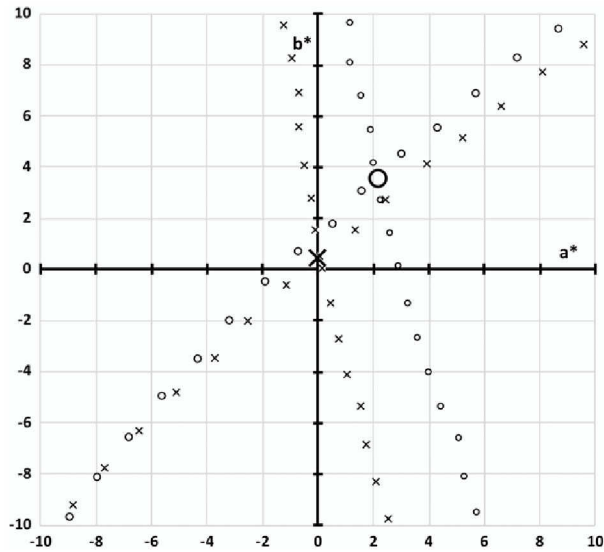


Figure 2. CIELAB b^* versus a^* plot of the reflectance data shown in Figure 1. The circle symbols were calculated using the CIE D50/2°, the x symbols with the CIE D50/10°. Large symbols show the match for each respective standard observer.

under the same source, and the closeness of those matches indicates the similarity of color vision of the observers.

Figure 1 shows spectral reflectance data of a D&H Color Rule. Figure 2 shows two sets of CIELAB data [7], both derived from the reflectance data shown in Fig. 1. The circles in Fig. 2 indicate the a^* and b^* coordinates calculated using CIE Standard Illuminant D50 and the CIE 1931 2° Standard Observer; the x's using CIE Standard Illuminant D50 and the CIE 1964 10° Standard Observer. What is of interest is the point of intersection (the match) between the two respective lines (red points). The color difference between these points, $4.0\Delta E_{00}$, is an indication of the difference between the 1931 and 1964 Standard Observers. A color difference is a familiar metric that we believe is more useful than spectral dissimilarity when plotting the two standard observers.

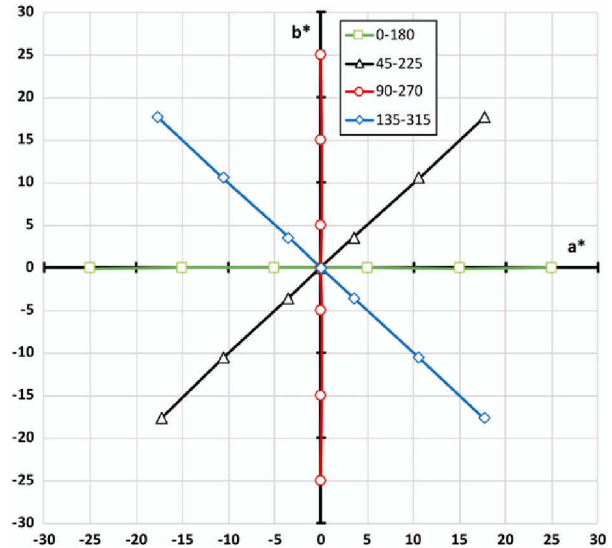


Figure 3. D50/2° CIELAB for the virtual target patches.

2.1 Virtual Target

Using the underlying theory of the D&H Color Rule, four sets of seven reflectance spectra each were formulated. The two-constant opaque form of Kubelka–Munk turbid media theory was used to predict matches using Golden Heavy Body artist acrylic dispersion paints. This model has been shown to have good accuracy [8]. Paint combinations were sought that spanned $\pm 25C_{ab}^*$ at a specific hue angle and produced spectra that would be sensitive to changes in observers. Four groups were formulated in unique vector directions, shown in Figure 3 for D50/2° as a CIELAB projection onto the a^*b^* axes. All the formulations had an $L^* = 70$. The four specific points for each set of patches are listed in Table I. Each set of paints is unique; their spectra are plotted in Figure 4. The identifiers (first row) are the hue angles of the endpoints. Each of Figs. 4(a)–(d) show six theoretical spectral reflectance factors calculated by mixing the pigments in the columns of Table I.

2.2 Camera Testing Procedures

Two cameras were tested for this research, selected because of different spectral sensitivities (shown below). Both are high quality devices in regular use in professional archiving laboratories. A reference target [9] was measured and imaged by both systems. From the reference measurements and the average RGB of the patches, a simple profile was created. The camera profile, transforming camera digital counts into tristimulus values is shown in Eq. (1):

$$\begin{bmatrix} \hat{X} \\ \hat{Y} \\ \hat{Z} \end{bmatrix} = \begin{bmatrix} R_X & G_X & B_X \\ R_Y & G_Y & B_Y \\ R_Z & G_Z & B_Z \end{bmatrix} \times \begin{bmatrix} D_R/D_{R,max} - D_{R,offset} \\ D_G/D_{G,max} - D_{G,offset} \\ D_B/D_{B,max} - D_{B,offset} \end{bmatrix}, \quad (1)$$

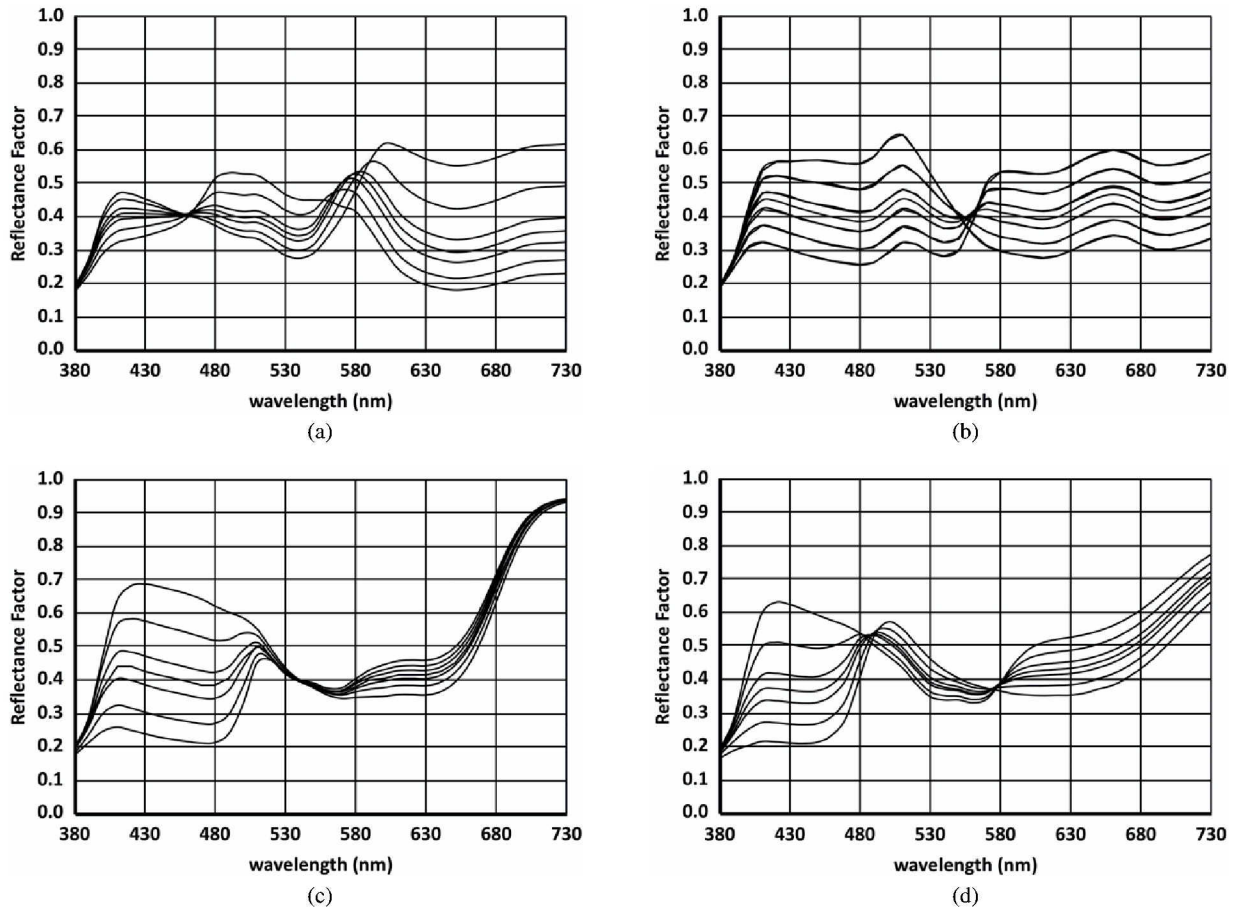


Figure 4. Reflectance spectra of four sets of the virtual target patches: (a) 0–180, (b) 45–225, (c) 90–270, and (d) 135–215. Each line represents a unique mixture of the pigments listed in the respective column of Table I.

Table I. Paints used for each set of patches.

Paint	0–180	45–225	90–270	135–315
1	Pyrrole orange		Arylide yellow	Bismuth vanadate yellow
2	Phthalocyanine green	Phthalocyanine blue	Cerulean blue	Ultramarine blue
3	Quinacridone magenta	Arylide yellow	Quinacridone magenta	
4	Titanium white			

where: D_R , D_G , and D_B are the mean patch digital counts; $D_{R,max}$, $D_{G,max}$, and $D_{B,max}$ are the maximum digital counts; and \hat{X} , \hat{Y} , and \hat{Z} are the estimated tristimulus values.

The 12 terms (3×3 RGB to XYZ transform matrix and channel offsets) were optimized where the objective function minimized the average $\Delta E_{00(SL=1)}$ color difference between the CIELAB coordinates calculated from the estimated tristimulus values and the reference CIELAB data from the measurements of the characterization target. The derived

matrix and offset parameters will be used for the camera modeling for the balance of this article.

In addition to the derivation of the camera model the relative spectral sensitivities for these two cameras were also measured. The technique is similar to that described in [10]. The spectral sensitivities will be used for the virtual imaging of the targets described in the next section. These sensitivities are shown in Figure 5. The red spectral sensitivities are quite different, often a cause of poor color accuracy. The simple camera model, shown in Eq. (2), assumes no internal matrix

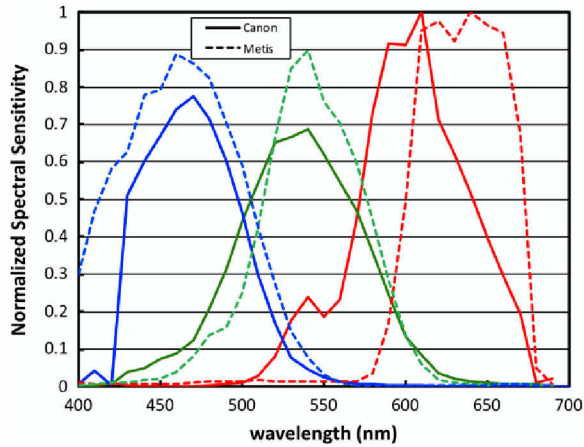


Figure 5. Relative spectral sensitivities for the two test cameras.

corrections or white balance:

$$DC_{R,i} = \frac{1}{\sum SS_{R,\lambda}} \sum_{\lambda} SS_{R,\lambda} R_{\lambda,i}, \quad (2)$$

where:

$DC_{R,i}$ is the normalized red digital count for the i th patch;
 $SS_{R,\lambda}$ is the spectral sensitivity of the red channel; and
 $R_{\lambda,i}$ is the spectral reflectance of the i th patch.

The green and blue channels are calculated similarly.

The cameras reported in this work are a Canon 1D Mark III and a Metis DRS2000 DCS large format flatbed scanner. Starting with Table II and thereafter, two additional camera configurations based on the Metis are reported. These will be described below in the section titled *Adjustment of Spectral Sensitivities*.

Table II. Color difference ($\Delta E_{00}SI = 1$) summary for the intersection points calculated using CIE 2°/D50. For reference the Vora and Trussell μ factor is also shown.

Camera	ΔE_{00} to CIE 2°/D50			Physical Target	Vora and Trussell μ factor
	Mean	Max	Std Dev		
Canon 1D	1.3	1.8	0.6	0.4	0.901
Metis	4.9	6.1	1.5	8.4	0.735
Metis+BG40	3.5	4.8	1.0	4.7	0.791
Metis+BG60	2.9	4.5	1.1	1.7	0.814

2.3 Testing Using Virtual Targets

The patch reflectances of the virtual target, shown in Fig. 4, were processed through the camera model in Eq. (2), and the resulting digital counts were further processed through the camera profile shown in Eq. (1). This yielded estimated tristimulus values, from which CIELAB coordinates were calculated in the usual fashion.

Figures 6(a,b) show the CIELAB results for the two cameras. These are analogous to the ideal results shown in Fig. 3 for the D50/2° data. The interesting aspect of Fig. 6(a,b) is the location of the six crossover points (black circles, shown for each combination). To mimic D50/2° perfectly, the crossovers should all be at the origin (as shown in Fig. 3 above). This is because the virtual target is designed to place the intersection of the four lines precisely at the origin (for D50/2° CIELAB). Therefore a deviation from this intersection point indicates that the camera deviates from the performance of D50/2° CIELAB. The cameras have markedly different rates of success toward this goal.

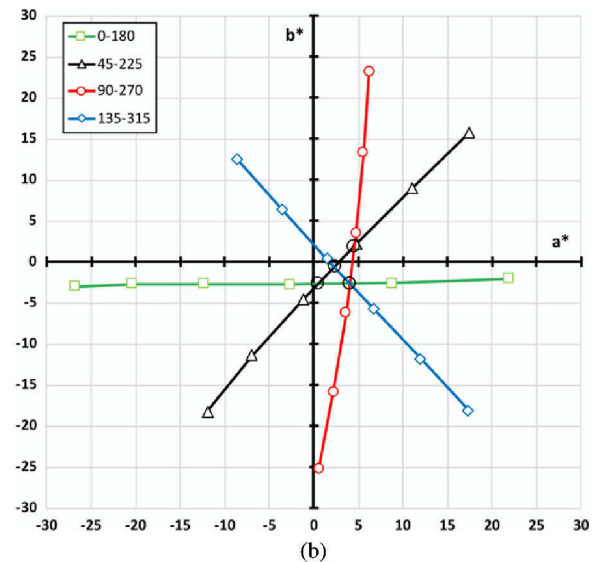
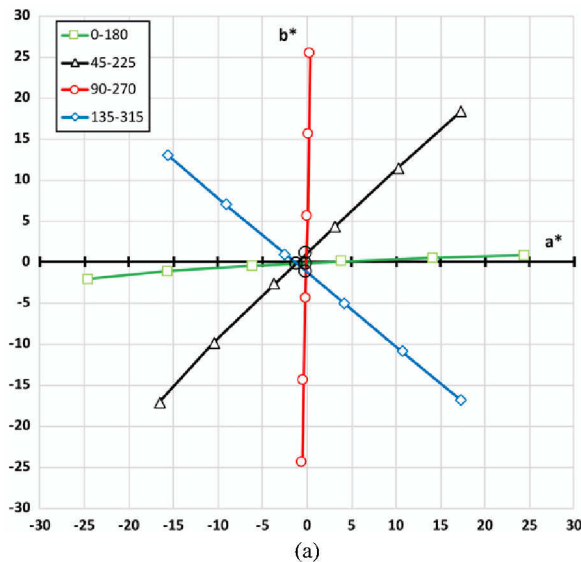


Figure 6. CIELAB data from the virtual targets for Canon 1D (a) and Metis flatbed scanner (b). The black circles are the six points of intersection for each combination of the four lines.

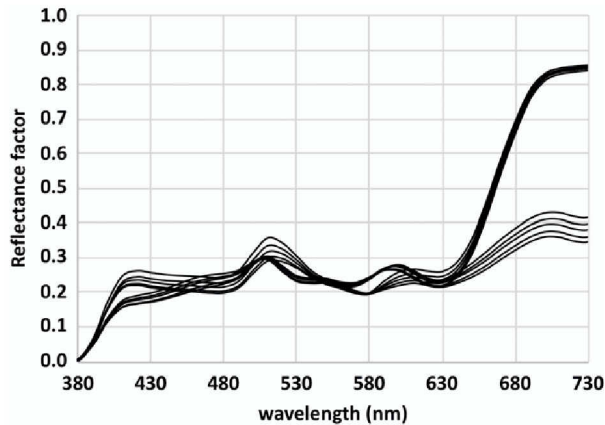


Figure 7. Spectral reflectance of the patches in the physical target "MCSL Spectral Target 3."

As a reasonable summary metric, the mean color difference for each of the seven points of intersection were calculated. The color difference results are shown in Table II.

2.4 Testing Using Physical Targets

A physical target with similar features to the virtual target has been produced. This target is designated "MCSL Spectral Target 3." Spectral reflectance and CIELAB data are shown in Figures 7 and 8, respectively. The color differences between the camera intersection points (large colored circles in Fig. 8) and CIE D50/2° (large black circle) are listed in Table II.

2.5 Adjustment of Spectral Sensitivities

Several of the results above make reference to the camera configurations "Metis+BG40" and "Metis+BG60." These

data are all based on a camera model (Eq. (2)) using spectral sensitivities that have been adjusted by pre-filtering all imagery with a light blue-green filter. This technique [11] alters the sensitivities to create more overlap between the green and red channels. Without the overlap the camera cannot distinguish between wavelengths above about 650 nm, where the green sensitivity drops to zero. The effect of the filters is to move the peak sensitivity of the red channel to a shorter wavelength, creating much more overlap with the green channel, and allowing the camera to better distinguish red wavelengths. Figure 9 shows the base and adjusted spectral sensitivities for the Metis scanner, as well as the transmittance of the two blue-green filters.

As can be seen by the results above, the pre-filtering improves the colorimetric accuracy of the Metis considerably.

3. DISCUSSION

The benefit of using these targets for camera analysis is that they do not require knowledge of a camera's spectral sensitivities. However, if known, it was of interest to compare this metamer approach with μ factor. Figure 10 shows the color differences from the various cameras and targets plotted against the μ factor for each camera. Symbol shape designates the camera configuration: open symbols are results from the virtual target, filled symbols are those from the physical target. The results reasonably correlate; linear fits have $R^2 = 0.99$ and 0.85 for virtual and physical targets, respectively. The reduced correlation for the physical target resulted from the samples not lying in a straight line in CIELAB.

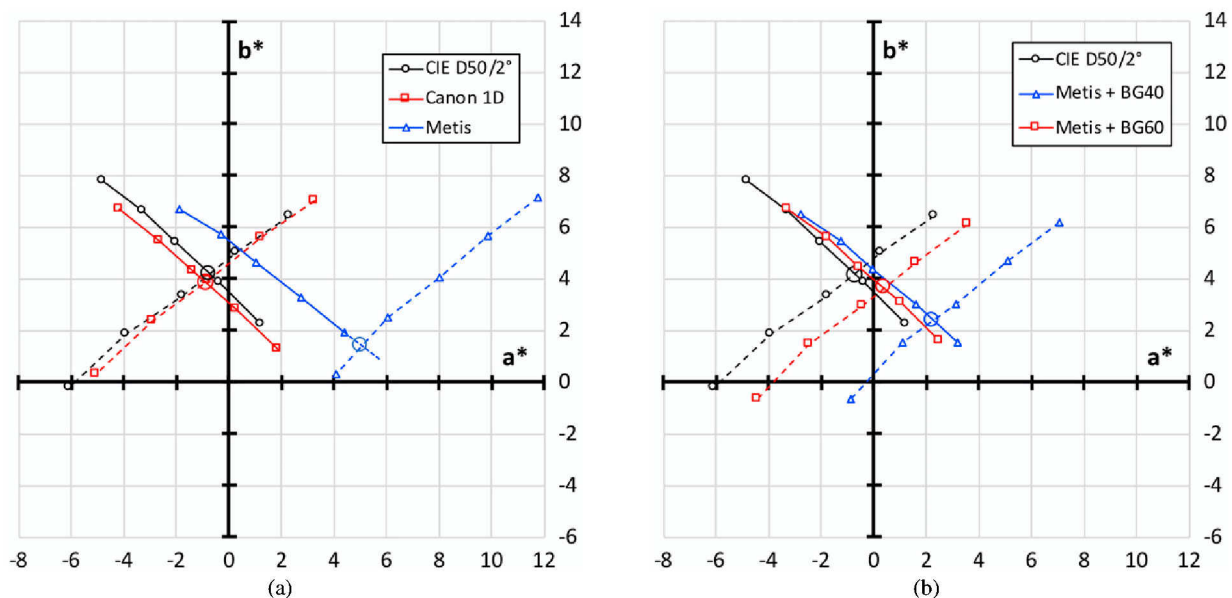


Figure 8. CIELAB b^* versus a^* projection for patches in the physical target "MCSL Spectral Target 3." Large circles show intersection points for each camera.

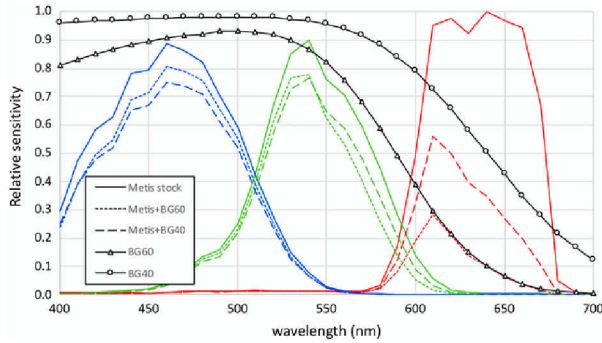


Figure 9. Base and adjusted spectral sensitivities for the Metis scanner (curves without symbols) and filter transmittances used to adjust those sensitivities (circle and triangle symbols). The solid colored curves are identical to the dotted curves in Fig. 4. The dashed and dotted curves show the effective spectral sensitivity after the filtering.

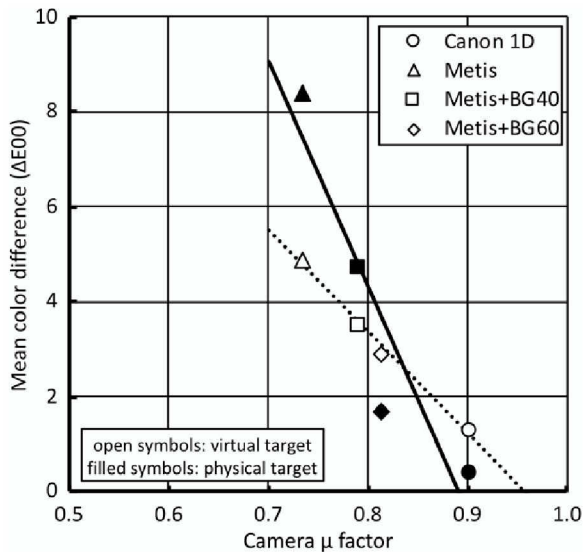


Figure 10. Comparison between μ factor and color difference for the camera and targets described here.

4. CONCLUSIONS AND FUTURE WORK

A new spectral camera target has been developed based on the theory underlying the D&H Color Rule. The purpose

of the target is to estimate the colorimetric accuracy of an imaging system (camera or scanner). It has been shown to correlate well with existing metrics designed to analyze spectral sensitivities, but the use of the new target does not require the complex procedures and instrumentation needed to measure sensitivities.

Future work should include a theoretical analysis of more cameras for which spectral sensitivities have been or will be measured, as well as empirical evaluation of the technique using a variety of cameras and light sources. The target also needs to be compared with traditional independent color targets. Additionally, the physical target may need to be augmented by adding patches formulated to be similar to the virtual targets described here. Finally, an analysis should be made to determine what levels of ΔE_{00} are required for various imaging applications.

REFERENCES

- 1 The latest ICC profile specification is ICC.2: 2017. Available for download from www.color.org.
- 2 S. Quan and N. Ohta, "Evaluating hypothetical spectral sensitivities with quality factors," *J. Imaging Sci. Technol.* **46**, 8–14 (2002).
- 3 P. L. Vora and H. J. Trussell, "Measure of goodness of a set of color-scanning filters," *J. Opt. Soc. Am. A* **10**, 1499–1508 (1993).
- 4 H. E. J. Neugebauer, "Quality factor for filters whose spectral transmittances are different from color mixture curves, and its application to color photography," *J. Opt. Soc. Am.* **46**, 821–824 (1956).
- 5 H. Hemmendinger and H. R. Davidson, "Color measurement in industry," *Proc. Symp. on Colour Measurement in Industry* (Imperial College, London, 1967).
- 6 J. Diaz, A. Chiron, and F. Viénot, "Tracing a metameric match to individual variations of color vision," *Color Res. Appl.* **23**, 379–389 (1998).
- 7 CIE No. 15. 2004, Colorimetry, Commission Internationale de l'Éclairage (2004).
- 8 R. S. Berns and M. Mohammadi, "Evaluating single- and two-constant Kubelka-Munk turbid media theory for instrumental-based inpainting," *Studies Conservation* **52**, 299–314 (2007).
- 9 Next Generation Camera Characterization Target, available from Avian Rochester, LLC www.NextGenTarget.com.
- 10 M. M. Darrodi, G. Finlayson, T. Goodman, and M. Mackiewicz, "Reference data set for camera spectral sensitivity estimation," *J. Opt. Soc. Am. A* **32**, 381–391 (2015).
- 11 R. S. Berns and S. Smith, "Analysis of color management default camera profiles for museum imaging applications," *Proc. IS&T Archiving 2012* (IS&T, Springfield, VA, 2012).